Proc. Natl. Acad. Sci. USA
Vol. 91, pp. 10360–10364, October 1994
Biophysics

Femtosecond coherent transient infrared spectroscopy of reaction centers from *Rhodobacter sphaeroides*

S. MAITI[†‡], G. C. WALKER[§¶], B. R. COWEN[§], R. PIPPENGER[§], C. C. MOSER[†], P. L. DUTTON[†], AND R. M. HOCHSTRASSER[§]

[§]Department of Chemistry and [†]The Johnson Research Foundation, University of Pennsylvania, Philadelphia, PA 19104

Contributed by R. M. Hochstrasser, June 20, 1994

ABSTRACT **Protein and cofactor vibrational dynamics associated with photoexcitation and charge separation in the photosynthetic reaction center were investigated with femtosecond (300–400 fs) time-resolved infrared (1560–1960 cm^{-1}) spectroscopy. The experiments are in the coherent transient limit where the quantum uncertainty principle governs the evolution of the protein vibrational changes. No significant protein relaxation accompanies charge separation, although the electric field resulting from charge separation modifies the polypeptide carbonyl spectra. The potential energy surfaces of the "special pair" P and the photoexcited singlet state P* and environmental perturbations on them are similar as judged from coherence transfer measurements. The vibrational dephasing time of P* modes in this region is 600 fs. A subpicosecond transient at 1665 cm^{-1} was found to have the kinetics expected for a sequential electron transfer process. Kinetic signatures of all other transient intermediates, P, P*, and P^+, participating in the primary steps of photosynthesis were identified in the difference infrared spectra.**

The reaction center (RC) protein contains about a thousand residues in three different subunits and has a molecular weight of ≈100,000. Two of the subunits, L and M, are related by an approximate C_2 symmetry (1–5). Each of these consists of seven transmembrane helices that span the ≈45-Å membrane lipid bilayer. Together these two subunits hold four bacteriochlorophyll a (BChl) molecules, two bacteriopheophytins (Bphs), two quinones (Q), and one nonheme iron atom. The C_2 axis passes through the iron atom (near the cytoplasmic side of the membrane) and through the midpoint of the line joining the centers of the two BChl molecules on the periplasmic side that are in van der Waals contact and constitute the "special pair" (P).

The primary kinetic event of the photosynthetic process consists of the transfer of an electron down the transmembrane chain of cofactors against the membrane potential using the energy of an absorbed photon (for a review, see ref. 6). Excitation of P creates the photoexcited singlet state (P*), which donates an electron to Bph_L to create the $P^+Bph_L^-$ state with a time constant of about 3 ps (for reviews, see refs. 7 and 8). Transfer of an electron from Bph_L to Q_A in about 200 ps creates the $P^+Q_A^-$ state, which generates the $P^+Q_B^-$ state in ≈100 μs.

The kinetics and energetics of most of the cofactors participating in this process were already characterized by spectroscopic techniques, but there are a number of unanswered questions. It is not yet clear why the electron is transferred to Bph_L and not Bph_M (refs. 9–11; for a review, see ref. 12). The increase of the rate of electron transfer at cryogenic temperatures (13–16) also is not explained. The dispersive kinetics observed in the first two steps of electron transfer (17) and the nonexponential primary electron transfer kinetics (18) are outstanding questions relating to the heterogeneity of the protein structure. Optically detected magnetic resonance experiments also point to heterogeneity in the RC population (for a review, see ref. 19). Ultrafast spectroscopic measurements exhibit vibrational coherence in as yet unassigned low-frequency modes having periods comparable with electron transfer times (20). Ultrafast kinetics obtained in the optical region have been interpreted to imply a one-step mechanism for electron transfer from P to Bph (21, 22), whereas Zinth and coworkers (23) have presented evidence for a two-step electron transfer scheme where P* reduces BChl in 2.8 ps and the $BChl^-$ species decays with a time constant of 0.8 ps to form P^+Bph^-. Theoretical calculations are not unequivocal as to the involvement of $BChl^-$ (24). Finally, information on the participation of the protein medium in the electron transfer is scarce.

Ultrafast vibrational spectroscopy is a natural approach to obtain answers to the foregoing questions. The protein IR absorbance before and after the electron transfer should manifest the changes that accompany the charge separation. Indeed studies of trapped intermediates (refs. 25–27; for a review, see ref. 28) have provided information on the vibrational states of the cofactors, their oxidized forms, and the protein. However, the measurement of changes in the IR absorbance with high sensitivity at pico- or subpicosecond time resolution (for reviews, see refs. 29 and 30) allows the time evolution and spectra of untrappable intermediates to be examined directly. This technique has been extended here to study the perturbations on the protein and cofactors resulting from the photoexcitation of P and the subsequent electron transfer steps, the time scale of protein response to charge separation, dephasing kinetics of vibrational modes affected by electron transfer, determination of vibrational linewidths, and the identity of the transient intermediates in the electron transfer pathway in the electron-transfer process.

METHODS

Time-Resolved IR. Change of absorbance in the vibrational IR due to photoexcitation of the RC was measured as a function of time with a resolution of 300–400 fs and IR frequency in the range 1560–1960 cm^{-1}. The electron transfer was initiated with a pulse of 870-nm light with energy 0.5 μJ and probed with a tunable carbon monoxide laser, which was gated (29, 30) by a short 870-nm pulse. The femtosecond pulses are generated by a mode-locked titanium: Al_2O_3 oscillator (MIRA-900; Coherent Radiation, Palo Alto, CA). A regenerative amplifier was constructed to amplify these low-

The publication costs of this article were defrayed in part by page charge payment. This article must therefore be hereby marked "*advertisement*" in accordance with 18 U.S.C. §1734 solely to indicate this fact.

Abbreviations: RC, reaction center; BChl, bacteriochlorophyll a; Bph, bacteriopheophytin.

[‡]Present address: Department of Applied and Engineering Physics, F-15, Clark Hall, Cornell University, Ithaca, NY 14853-2501.
[¶]Present address: Department of Chemistry, University of Pittsburgh, Pittsburgh, PA 15260.

energy (≈8 nJ) pulses to ≈10 μJ at a repetition rate of 5 kHz. More detail of this experiment is given in ref. 31.

The anisotropy after optical excitation was obtained from probe absorbance changes with the probe polarization parallel ($I_{\parallel}$) and perpendicular ($I_{\perp}$) to the pump polarization. The anisotropy is given by $(I_{\parallel} - I_{\perp})/(I_{\parallel} + 2I_{\perp})$, which is related to the angle θ between the pumped and probed transition dipoles (29). When there is a sharp equilibrium distribution of angles and rotational reorientation of the probed transition does not occur within the few first picoseconds, the anisotropy can be directly compared with the angles found from the x-ray structure assuming the carbonyl IR transitions are polarized along the relevant C—O bond. Theoretical calculations (32) of the polarization of the pump transition are used for estimating these angles.

Sample Preparation. RCs were isolated from photosynthetically grown *Rhodobacter sphaeroides* strain R-26 by the method of Clayton and Wang (33), using the detergent lauryldimethylamine oxide to solubilize the photosynthetic membranes. RC was further purified by fast protein liquid chromatography (FPLC) to an absorbance ratio of 280 to 802 nm of between 1.2 and 1.4. Bulk ^1H_2O was exchanged for ^2H_2O by repeated dilution of 10 mM Tris, pH 8 in ^2H_2O/0.04% lauryldimethylamine oxide/1 mM dithiothreitol and centrifugal Amicon filter concentration to about 1 mM final protein concentration. RC was placed between CaF_2 windows in a rotating thin cell.

Theory of the Spectral Response. The spectra are interpreted on the basis of a simple model in which the signal depends on the linewidths, absorption coefficients, and frequencies of the transitions involved as well as on the intensity envelope of the pumping and gating pulses and the frequency of the IR probe field. These properties are used to calculate the density matrix in terms of the vibrational states of the cofactors and protein (ref. 31; for a review, see ref. 30). At each IR frequency, the effect of all the nearby transitions is incorporated in the fits to the spectra. The diagonal elements of the density matrix (populations) were obtained from standard kinetic analysis of the models. It was assumed that the electronic dephasing is much faster than the experimental time resolution and that there is no transfer of vibrational coherence from P* to the products P^+, $BChl^-$, or Bph^-. The theoretical approach includes optically induced coherence transfer between P and P*. These assumptions are justified *a posteriori* by observations of the transients. Because the method uses gating of a continuous wave IR field, the signals are not the same as those that would be observed with short IR pulses.

RESULTS

The 1590- to 1790-cm^{-1} frequency range encompasses the amide I band of backbone carbonyl stretch vibrations of the protein (34): P, BChl, and Bph all have carbonyl groups that absorb in this region. The spectrum is therefore sensitive to conformational and electrostatic changes of all parts of the RC complex. Kinetics were measured every 4–8 cm^{-1} in this frequency range. Fig. 1 shows the difference absorption spectrum plotted at four representative time delays. The largest absorption change measured, at 1702 cm^{-1}, was 0.5% of the peak static absorbance of the sample. The total area under the difference spectrum at 35 ps is 0.3% of the area under the static absorbance spectrum.

Fig. 2*A* shows a three-dimensional plot of data between −2 and +5 ps in the time axis and 1694 and 1714 cm^{-1} in the frequency axis. This strong difference band was identified with the 9-keto C=O group of P^+ in earlier studies (35, 36). Fig. 2*B* shows the kinetics at separate frequencies in this region. The fits establish that a 9-cm^{-1} bandwidth transition is shifting from 1682 cm^{-1} (see below) to 1702 cm^{-1} with a time constant of 2.5 ps.

Fig. 3 shows the kinetics obtained at 1682 cm^{-1}. A bleaching of the ground-state population, accompanied by an initial increase in absorbance, is observed. The bleach corresponds to the 9-keto C=O group of the neutral P (35, 36). The positive component has the kinetic characteristics of an electronic absorption band of the special pair P* and P^+ states (37). A sum of two exponentials are used for the positive component; the first rises instantaneously with the excitation and decays with a time constant of 2.5 ps (P* electronic absorption), and the second component rises with a time constant of 2.5 ps to a plateau.

Fig. 4 shows the kinetics obtained at 1665 cm^{-1}. A significant contribution from a transient species is evident, along with the formation of a population that does not decay. The transient signal exhibits a rise time in the range of 1 ps. Two kinetic models, one involving a population of the $Bchl_L^-$ species and the other ignoring it, are used to obtain the two different fits shown in the figure (see below for discussion).

The kinetics at 1612 cm^{-1} (not displayed, other than the four points in Fig. 1) show a large contribution from a transient species, along with the formation of a stationary population. The rise time (<0.4 ps) of the transient signal signifies a different component of the RC from that observed at 1665 cm^{-1}. It is tentatively identified with part of an electronic absorption band of the special pair P* and underlying P^+ states.

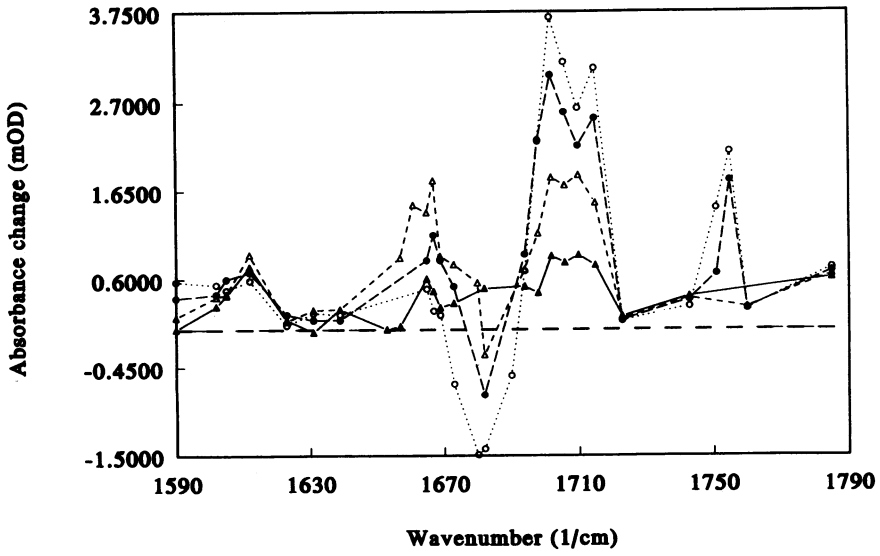

FIG. 1. Difference absorbance spectrum of the RC at four representative time delays of 1 ps (▲), 2.5 ps (△), 5 ps (●), and 35 ps (○). The dashed horizontal line represents zero absorbance change. Points have been joined by straight lines for clarity. OD uncertainty is ≤0.25 × 10^{-3} (mOD).

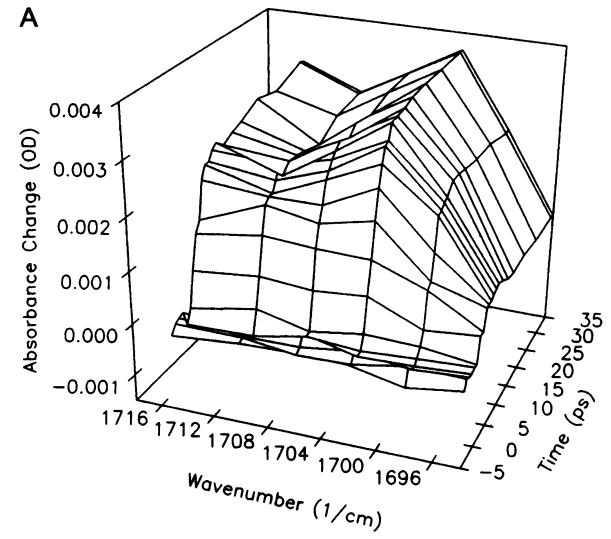

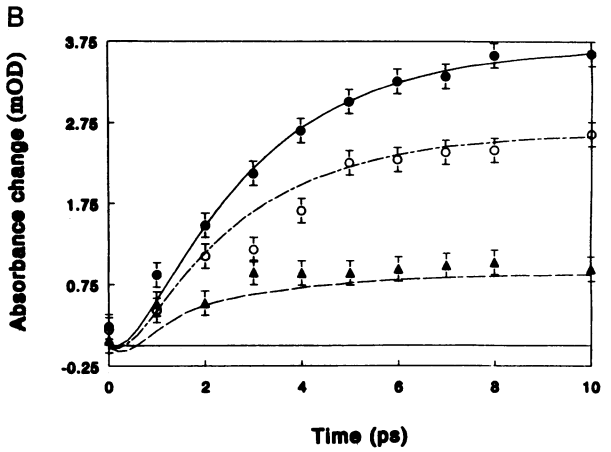

FIG. 2. (*A*) Kinetics in the 1702-cm^{-1} region in a three-dimensional plot. Uncertainty is ≤0.2 mOD. Points are joined by straight lines for clarity. (*B*) Least-squares fits to the kinetics at 1702 cm^{-1} (●), 1698 cm^{-1} (○), and 1694 cm^{-1} (▲) include dephasing-limited kinetics of the P, P*, and P$^+$ species. The electron transfer time and the width of Lorenzian vibrational lines are free parameters.

As noted previously (36) the change in absorbance is mainly positive, indicating that the transitions of P* and P$^+$ are stronger than those for P. Anisotropies were measured for

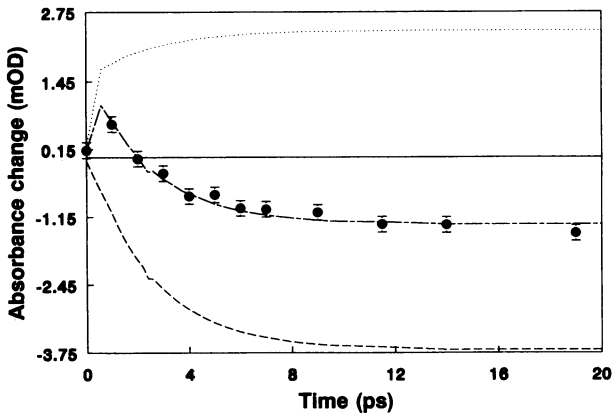

FIG. 3. Kinetics at 1682 cm^{-1}. The fit (●) is a sum of a vibrational bleach (dashed line) and an electronic absorption of the P* and (perhaps) P$^+$ states (dotted line).

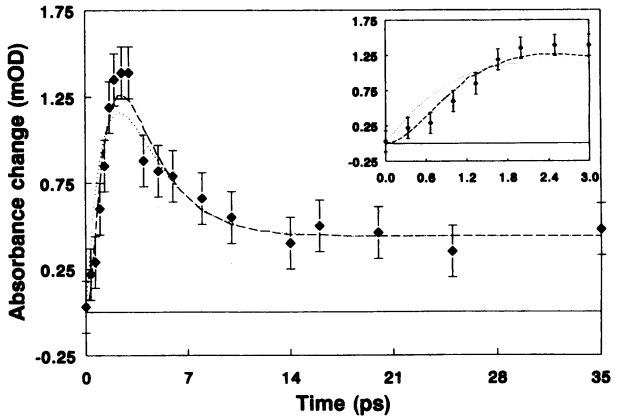

FIG. 4. Kinetics at 1665 cm^{-1}. The fits are sums of an absorbance of a transient species and of a P/P$^+$ difference spectrum. One fit assumes the transient species to be BChl$^-$ (dashed line); the other assumes it to be P* (dotted line) with a 5-cm^{-1} linewidth. (*Inset*) Expanded view of the first 3 ps.

most bands, and they were all time independent, confirming that there is no motion of the cofactor transition dipoles on the time scale of 0.3–3.5 ps.

DISCUSSION

Understanding the Kinetics of Specific Spectral Regions. The method of time-gated detection employs spectral resolution narrower than the vibrational bandwidths and temporal resolution shorter than the dephasing time associated with these linewidths (29, 30). Under these conditions, the signal evolution depends on the kinetics and on the shift and the width of the vibrational transitions being probed.

The 9-Keto Vibration of P$^+$: The 1702-cm^{-1} Region. A broad band with two peaks at 1702 and 1714 cm^{-1} is the strongest feature observed in the difference spectrum. This band has been assigned to the two 9-keto groups of P_L and P_M of the oxidized special pair (25, 36). The anisotropy at 1702 cm^{-1} was 0.19 ± 0.04, so it was assigned as the P_M 9-keto carbonyl (expected anisotropy, 0.2). The 1714-cm^{-1} peak is therefore identified as the 9-keto of P_L or is associated with some other vibration of the P$^+$ or Bph$^-$ species (see later). Stark effect (38, 39), electron neutron double resonance spectroscopy (40), and Fourier transform IR (41) measurements also indicate an asymmetric electrostatic environment for P_L and P_M.

A distribution of rise times from 1.8 to 3.0 ps is found across the ≈10-cm^{-1}-wide band (half-width at half-maximum) at 1702 cm^{-1}. A distribution of electron transfer rates in the RC is not needed to explain this result since, when vibrational dephasing is included, the kinetics with a uniform electron transfer rate is predicted to be nonexponential with different rise times at different frequencies. With the 9-keto bands of P and P$^+$ centered at 1682 and 1702 cm^{-1}, the least-squares fit yields a vibrational dephasing time of 600 fs and an electron transfer time of 2.5 ps** (Fig. 2*B*).

The 9-Keto Vibration of P: The Bleach Around 1680 cm^{-1}. The initial, small positive component of the kinetics in Fig. 3 implies that the band being probed is broader than ≈50 cm^{-1}, which may correspond to an electronic transition of P* at

**We have observed examples of heterogeneity that are not revealed in the visible spectra. For example, samples studied at the very outset of this research exhibited an additional (70%) long time (10 ps) component to the transient adsorption of the 9-keto at 1702 cm^{-1}. In these samples, this component correlated with 10 ps reorientational dynamics at the adjacent 10*a* ester at 1755 cm^{-1}. The samples in the present research did not show these effects.

even lower frequency than the electronic transition reported previously (37). It now appears likely that a weak electronic absorption spectrum could underlie the vibrational spectrum over the whole region 1560–1960 cm^{-1}. The negative component of the signal, due to the bleach of the 9-keto carbonyl vibration of P, grows in over a few picoseconds. The time evolution of the bleach should be very sensitive to the changes in width and frequency of the vibrational transition on excitation of P. The fact that the 9-keto vibrational band of P does not disappear in synchrony with the disappearance of P population implies that the vibrational coherence is retained even as the electronic state changes from P to P*. We conclude that the width and frequency of this 9-keto mode are *not* changed significantly on excitation of $P \rightarrow P^*$, implying very similar potential surfaces for these two states. The similar dephasing times of 600 fs for P and P* implies that the environmental perturbations are similar in both states.

The Amide I Region: Ultrafast Transient at 1665 cm^{-1}. The spectral kinetics in the region of 1661 to 1669 cm^{-1} reveals the existence of a transient species with a lifetime shorter than a few ps. In bacterial photosynthesis, only two intermediates have such short lifetimes, so this signal must be connected with either or both of them. One is the electronically excited state of the special pair (P*), which decays with the formation of P^+ in 2–3 ps. The other is the reduced accessory bacteriochlorophyll on the L side ($BChl^-$). It has been proposed that $BChl^-$ forms with the formation of P^+ in 3.5 ps and decays with the formation of Bph^- in 0.9 ps (23). Other possibilities for transitions in this region include the 2*a* acetyl or 9-keto carbonyls of the cofactors and the amide carbonyls of the protein backbone responding to either or both of the aforementioned processes. The kinetics allow us to test for the existence of a population of $BChl^-$.

The kinetics at 1665 cm^{-1} shown in Fig. 4 was fit to the expected time-dependent absorbance change of a carbonyl stretching mode that shifts in frequency by 20 cm^{-1} when perturbed by P* or $BChl^-$. The signal levels off at a finite positive value, implying a contribution from the P^+Bph^- species. The relative magnitudes of the transient and the persistent components of the signal are the two free parameters of the fit. The width of the band is fixed at 9 cm^{-1}, and the electron transfer time is fixed at 2.5 ps in accordance with the values found earlier for the 9-keto band. The peak frequency is chosen to be the center frequency of the observed band—namely, 1665 cm^{-1}. The fits to the P* kinetics (see Fig. 4) were systematically poorer than those to the $BChl^-$ kinetics. The best possible P* fit required an unphysically long dephasing time of 3.6 ps. For the $BChl^-$ model, the lifetime of $BChl^-$, which was varied as a free parameter, was found to be 0.9 ps for the best fit. The fits to the data are shown in Fig. 4 (*Inset* shows an expanded view of the first few picoseconds). The number of data points and the signal-to-noise ratio at the adjacent frequencies (1667 and 1669 cm^{-1}) are more limited, but the $BChl^-$ kinetics consistently fit the data better.

The anisotropy measured at 1667 cm^{-1} at a time delay of 2.5 ps was 0.25 ± 0.08. The expected anisotropy for the 9-keto of $BChl_L^-$ is 0.36. The underlying amide I response (48% of the signal at 2.5 ps) will reduce this somewhat, so that the observations are consistent with expectations for $BChl^-$. The sequential electron transfer scheme with $BChl^-$ as a kinetic intermediate (23) is therefore supportable by this result. The average calculated anisotropy of a signal from the amide I carbonyls within a 1-nm radius of P is −0.09. Thus perturbation of amide carbonyl(s) resulting from the presence of P* is excluded. The 2*a* acetyl C=O of P_M also would have too small an anisotropy (0.14).

A number of facts argue against the $BChl^-$ interpretation. The intensity of the 1665-cm^{-1} transient is larger than expected for a $BChl^-$ carbonyl, which, because of the fast decay, can only achieve 20% of its possible value. Its total signal area at 2.5 ps is about 40% of that at 1702 cm^{-1}. Mäntele and coworkers (25) have shown that the IR cross sections for the same mode in neutral, cationic, and anionic species can vary by a factor of 4. The frequency of the 9-keto vibration of $BChl^-$ is 1645 cm^{-1} in tetrahydrofuran solution, but shifts of 20 cm^{-1} are known to occur between such solutions and protein (42). Thus, the association of the transient at 1665 cm^{-1} with $BChl^-$ is not excluded by experiments on separated cofactors. The assignment of the fast 1665-cm^{-1} signal to $BChl^-$ would require that an incoherent population of this species is established faster than 900 fs. This is not in accord with expectations from some theoretical predictions of the ordering of P* and $BChl^-$ states (43) nor with simulations based on these calculations (ref. 44 and references therein) in which the $BChl^-$ state is placed at higher energy than P*. A study of the 1665-cm^{-1} region with IR probe pulses is needed to distinguish clearly P* from $BChl^-$.

The Response of the Protein. In the 1665-cm^{-1} region, where the fast transient occurs, there is a slower component that grows in 2.5 ps and remains constant thereafter. We attribute this signal to the amide I response (37): there are no P^+ transitions seen in this region. A protein conformational change or a vibrational Stark effect might cause this apparent intensity increase of the amide transitions.

It is proposed that the observed signal is from a large number of amide oscillators experiencing small vibrational Stark shifts and intensity changes as a result of the electrostatic fields associated with the primary charge separation. Using the procedures of Sharp and coworkers (45), we calculated the electric field at each carbonyl of the protein (31) and then by means of quantum chemical calculations (42) on formaldehyde estimated vibrational spectral shifts in the range -2 to 2 cm^{-1} and an average intensity of 0.17%. Such changes are adequate to account qualitatively for the observation of a 0.05% increase in the intensity. There is no evidence of a large-scale protein conformational change during the first 35 ps of photosynthesis from which shifts in the range of $\approx$15 cm^{-1} can be expected (34). This result is consistent with a number of other experiments (46, 47).

Significant differences exist in both the amide I and cofactor regions of the spectra reported here and those of dry lipid films (37). These two preparations are known to differ functionally, with the most noticeable differences being the absence of a peak around 1640 cm^{-1}, a much diminished feature around 1660 cm^{-1}, and the presence of a band around 1700 cm^{-1} in the solution RC. Both the 1640- and the 1665-cm^{-1} region are expected to be dominated by protein amide I changes. Thus the overall change in the vibrational spectrum of the protein on electron transfer from $P \rightarrow Bph$ is even smaller in the solution RC compared with the dry film preparation. The likely reason is the presence of intraprotein water molecules (35), which effectively shield the ionic charges from the rest of the protein medium in the solution preparation and also stabilize the charge-separated state.

CONCLUSIONS

This femtosecond IR study addresses how the vibrational transitions respond to the primary electronic processes. Two global issues concern the increased absorption across the spectrum after excitation and the absence of large protein relaxation after charge separation. There are protein signatures to be seen in the spectrum, but we suggest they are attributable to electric field effects on the polypeptide carbonyls—effects that result in negligible energy reorganization. The potential energy surfaces and environmental perturbations for P and P* are very similar based on a mode having the same dephasing time and frequency in both states.

The excited state (P*) dephasing time for this mode is 600 fs, which is just somewhat shorter than the time (≈2.5 ps) for electron transfer. A transition at 1665 cm^{-1} has time dependence consistent with a population of accessory bacteriochlorophyll being formed with kinetics in agreement with those reported by Zinth and coworkers (23). The attribution of this band to a P* transition could not be ruled out although a definitive experiment was proposed. The anisotropy measurements have shown that the strong carbonyl vibration at 1702 cm^{-1} is associated with the P_M side of the special pair, indicating that significant charge alteration occurs on the M side after electron transfer. Comparison with IR spectra of dried films suggests participation of intraprotein water in the reorganization associated with electron transfer.

We thank G. Sandrasegaram for his help with the Stark effect calculations. This research was supported by National Institutes of Health and National Science Foundation grants to P.L.D. and R.M.H., National Institutes of Health Postdoctoral Fellowships to B.R.C. and G.C.W., and the University of Pennsylvania Laser Facility (National Institutes of Health Grant RR 01348).

1. Deisenhofer, J., Epp, O., Miki, K., Huber, R. & Michel, H. (1984) *J. Mol. Biol.* **180**, 385–398.
2. Deisenhofer, J., Epp, O., Miki, K., Huber, R. & Michel, H. (1985) *Nature (London)* **318**, 618–624.
3. Deisenhofer, J. & Michel, H. (1988) in *The Photosynthetic Bacterial Reaction Center: Structure and Dynamics*, NATO ASI Series 149, eds. Breton, J. & Vermeglio, A. (Plenum, New York), pp. 1–12.
4. Chang, C. H., Tiede, D., Tang, J., Smith, U., Norris, J. R. & Schiffer, M. (1986) *FEBS Lett.* **205**, 82–86.
5. Yates, T. O., Komiya, H., Chirino, A., Rees, D. C., Allen, J. P. & Feher, G. (1988) *Proc. Natl. Acad. Sci. USA* **85**, 7993–7997.
6. Lehninger, A. L., Nelson, D. L. & Cox, M. M. (1993) *Principles of Biochemistry* (Worth, New York).
7. Kirmaier, C. & Holten, D. (1993) in *The Photosynthetic Reaction Center*, eds. Deisenhofer, J. & Norris, J. (Academic, New York), Vol. 2, pp. 49–70.
8. Zinth, W. & Kaiser, W. (1993) in *The Photosynthetic Reaction Center*, eds. Deisenhofer, J. & Norris, J. (Academic, New York), Vol. 2, pp. 71–86.
9. Kellogg, E. C., Kolaczkowski, S., Wasielewski, M. R. & Tiede, D. M. (1989) *Photosynth. Res.* **22**, 47–59.
10. Bylina, E. J., Kirmaier, C., Mcdowell, L., Holten, D. & Youvan, D. C. (1988) *Nature (London)* **336**, 182–184.
11. Chan, C.-K., Chen, L. X.-Q., Dimagno, T. J., Hanson, D. K., Nance, S., Schiffer, M., Norris, J. R. & Fleming, G. R. (1991) *Chem. Phys. Lett.* **176**, 366–372.
12. Dimagno, T. J. & Norris, J. R. (1993) in *The Photosynthetic Reaction Center*, eds. Deisenhofer, J. & Norris, J. (Academic, New York), Vol. 2, pp. 105–127.
13. Devault, D. & Chance, B. (1966) *Biophys. J.* **6**, 825–847.
14. Kirmaier, C., Holten, D. & Parson, W. W. (1985) *Biochim. Biophys. Acta* **810**, 33–48.
15. Kirmaier, C., Holten, D. & Parson, W. W. (1985) *Biochim. Biophys. Acta* **810**, 49–61.
16. Fleming, G. R., Martin, J. L. & Breton, J. (1988) *Nature (London)* **333**, 190–192.
17. Kirmaier, C. & Holten, D. (1990) *Proc. Natl. Acad. Sci. USA* **87**, 3552–3556.
18. Du, M., Rosenthal, S. J., Xie, X. L., Dimagno, T. J., Schmidt, M., Norris, J. R. & Fleming, G. R. (1992) *Proc. Natl. Acad. Sci. USA* **89**, 8517–8521.
19. Hoff, A. J. (1993) in *The Photosynthetic Reaction Center*, eds. Deisenhofer, J. & Norris, J. (Academic, New York), Vol. 2, pp. 331–382.
20. Vos, M. H., Rappaport, F., Lambry, J. C., Breton, J. & Martin, J. L. (1993) *Nature (London)* **363**, 320–325.
21. Kirmaier, C. & Holten, D. (1991) *Biochemistry* **30**, 609–613.
22. Lockhart, D. J., Kirmaier, C., Holten, D. & Boxer, S. G. (1990) *J. Phys. Chem.* **94**, 6987–6995.
23. Arlt, P., Schmidt, S., Kaiser, W., Lauterwasser, C., Meyer, M., Scheer, H. & Zinth, W. (1993) *Proc. Natl. Acad. Sci. USA* **90**, 11757–11761.
24. Bixon, M., Jortner, J. & Michel-Beyerle, M. E. (1992) in *The Photosynthetic Bacterial Reaction Center II: Structure, Spectroscopy and Dynamics*, NATO ASI Series A237, eds. Breton, J. & Vermeglio, A. (Plenum, New York), pp. 291–300.
25. Mäntele, W., Wollenweber, A. M., Nabedryk, E. & Breton, J. (1988) *Proc. Natl. Acad. Sci. USA* **85**, 8468–8472.
26. Buchanan, S., Michel, H. & Gerwert, K. (1992) *Biochemistry* **31**, 1314–1322.
27. Morita, E. H., Hayashi, H. & Tasumi, M. (1991) *Chem. Lett.* **9**, 1583–1586.
28. Mäntele, W. (1993) in *The Photosynthetic Reaction Center*, eds. Deisenhofer, J. & Norris, J. (Academic, New York), Vol. 2, pp. 239–277.
29. Locke, B., Diller, R. & Hochstrasser, R. M. (1993) in *Biomolecular Spectroscopy*, eds. Clark, R. J. H. & Hester, R. E. (Wiley, New York), pp. 1–47.
30. Hochstrasser, R. M. (1994) in *Monographs on Chemistry in the 21st Century Series*, IUPAC, ed. El-Sayed, M. A. (Blackwell, Oxford).
31. Maiti, S. (1994) Ph.D. thesis (Univ. of Pennsylvania, Philadelphia).
32. Warshel, A. & Parson, W. W. (1987) *J. Am. Chem. Soc.* **109**, 6143–6152.
33. Clayton, R. K. & Wang, R. T. (1971) *Methods Enzymol.* **23**, 696–704.
34. Krimm, S. & Bandekar, J. (1986) *Adv. Protein Chem.* **38**, 181–364.
35. Beroza, P., Fredkin, D. R., Okamura, M. Y. & Feher, G. (1992) in *The Photosynthetic Bacterial Reaction Center II: Structure, Spectroscopy and Dynamics*, NATO ASI Series A237, eds. Breton, J. & Vermeglio, A. (Plenum, New York), pp. 363–374.
36. Maiti, S., Cowen, B. R., Diller, R., Iannone, M., Moser, C. C., Dutton, P. L. & Hochstrasser, R. M. (1993) *Proc. Natl. Acad. Sci. USA* **90**, 5247–5251.
37. Walker, G. C., Maiti, S., Cowen, B. R., Moser, C. C., Dutton, P. L. & Hochstrasser, R. M. (1994) *J. Phys. Chem.* **98**, 5778–5783.
38. Lockhart, D. J. & Boxer, S. G. (1988) *Proc. Natl. Acad. Sci. USA* **85**, 107–111.
39. Losche, M., Feher, G. & Okamura, M. Y. (1987) *Proc. Natl. Acad. Sci. USA* **84**, 7537–7541.
40. Mattioli, T. A., Robert, B. & Lutz, M. (1992) in *The Photosynthetic Bacterial Reaction Center II: Structure, Dynamics and Spectroscopy*, NATO ASI Series A237, eds. Breton, J. & Vermeglio, A. (Plenum, New York), pp. 127–132.
41. Breton, J., Nabedryk, E. & Parson, W. W. (1992) *Biochemistry* **31**, 7503–7510.
42. Andres, J. L., Marti, J., Duran, M., Lledos, A. & Bertran, J. (1991) *J. Chem. Phys.* **95**, 3521–3527.
43. Thompson, M. A. & Zerner, M. C. (1991) *J. Am. Chem. Soc.* **113**, 8210–8215.
44. Gehlen, J. N., Chandler, D. & Marchi, M. (1993) *J. Am. Chem. Soc.* **115**, 4178–4190.
45. Anni, H., Vanderkooi, J., Sharp, K., Yonetani, T., Hopkins, S., Herenyi, L. & Fidy, J. (1994) *Biochemistry* **33**, 3475–3486.
46. Fischer, M. R., De Groot, H. J., Raap, J., Winkel, C., Hoff, A. J. & Lugtenburg, J. (1992) *Biochemistry* **31**, 11038–11049.
47. Fleming, G. R. & Van Grondelle, R. (1994) *Physics Today*, Feb. 1994, 48–55.